

The Magnetic Flux Leakage Inspection of Wire Ropes

Herbert R. Weischedel
NDT Technologies, Inc.

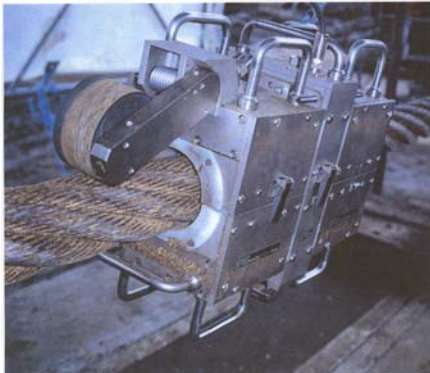
Introduction

Because the reliable and safe use of wire ropes is crucial for many mining, oil industry, crane and ski lift operations, concern with their integrity is a constant preoccupation of users and safety authorities. In spite of these concerns, a frequent reluctance to apply appropriate wire rope inspection methods and retirement criteria compromise safety in many cases. On the other hand, more dependable inspection methods and instrumentation are now available. These more effective procedures, combined with a better understanding of degradation mechanisms and discard criteria, can notably increase wire rope safety.

For example, advanced electromagnetic (EM) wire rope inspection equipment of the magnetic flux leakage (MFL) type has been developed over the past few decades. These instruments provide an important and in many cases indispensable element of wire rope inspection.

Two different and distinct EM methods have evolved for the detection and measurement of rope defects

FIGURE 1. Mooring rope inspection



- *Loss of Metallic Cross-Sectional Area (LMA) Inspection*, which (quantitatively) measures loss of metallic cross-sectional area caused by external or internal corrosion (due to environmental conditions or poor lubrication) and wear (due to rubbing along floors, nicking, high pressures, and/or poor lubrication).
- *Localized-Flaw (LF) Inspection*, which (qualitatively) detects a wide variety of external and internal discontinuities such as broken wires and corrosion pitting. Broken wires are usually caused by fatigue, interstrand nicking and martensitic embrittlement.

Modern dual-function EM rope testers allow simultaneous LMA and LF inspections. Figure 1 shows the EM inspection of an oil platform mooring rope.

Underlying Principles

For all present dual-function instruments, strong permanent magnets induce a magnetic flux at the saturation level in the rope in the axial (longitudinal) direction. Various types of sensors, such as coils, Hall sensors or fluxgate sensors close to the rope sense and measure the magnetic flux.

Any discontinuity – such as a broken wire or corrosion pitting – distorts the magnetic flux in the rope and causes it to leak from the rope. For LF inspections, the *radial* component of the leakage flux is measured by so-called *radial* sensors. Note that these sensors are also called *differential* sensors because they sense only changes of the magnetic flux in the rope and not the flux itself. Therefore, flaw detection depends on a rapid change of the magnetic flux, which is typically caused by broken wires and corrosion pitting. Differential sensors cannot detect more gradual changes of the rope flux, which are typically caused by wear and corrosion.

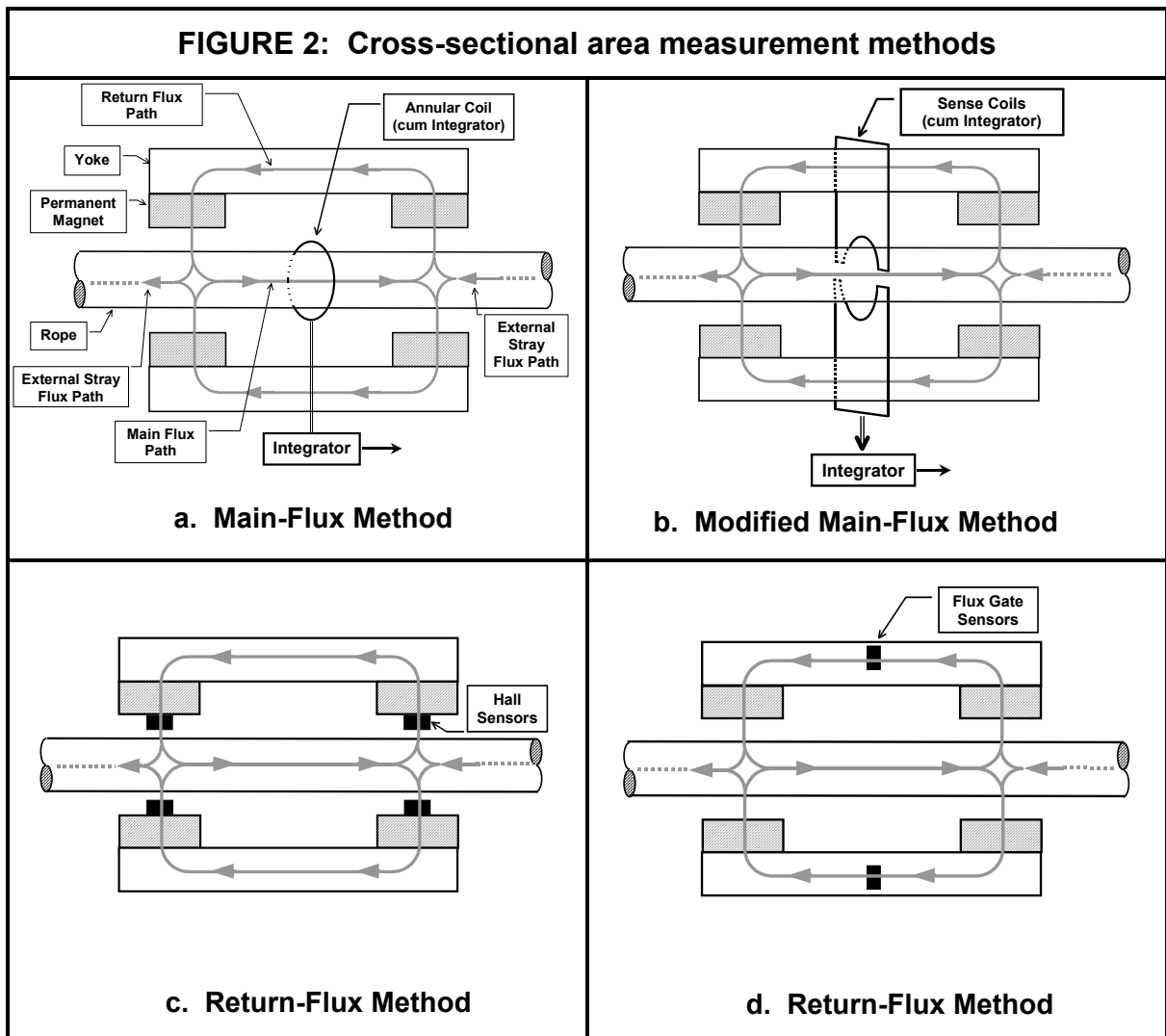
The *axial* component of the leakage flux can be measured by *axial* sensors. This *axial* leakage flux signal is frequently offered as a substitute for the LMA signal. However, while the *axial* signal can be useful for qualitative defect characterization, it is very complex and cannot be directly used to determine the LMA of a rope. Therefore, instruments that use this approach are not of the dual-function type as defined above. Methods for the (quantitative) measurement of the LMA of a rope are discussed below.

When a rope is magnetically saturated, the axial magnetic flux in the rope is proportional to its cross-sectional area. Therefore, any LMA can be determined by measuring this magnetic flux. Two types of sensors can be used to measure magnetic flux: Hall sensors (or, alternatively, fluxgate sensors) and coils in combination with electronic integrator circuits.

To measure flux density, Hall sensors (and fluxgate sensors) must be physically inserted directly into the magnetic flux path. Thus, the flux to be measured must intersect the sensors. This is not possible when measuring the magnetic flux inside the rope. Therefore, instruments that use Hall sensors or fluxgate sensors must always resort to an indirect method for determining the axial rope flux. They measure some flux density outside the rope and determine or estimate the longitudinal rope flux from the external flux measurement.

Alternatively coils-cum-integrators can be used. Because coils must encircle the magnetic flux to be measured, they can directly measure the magnetic flux inside the rope.

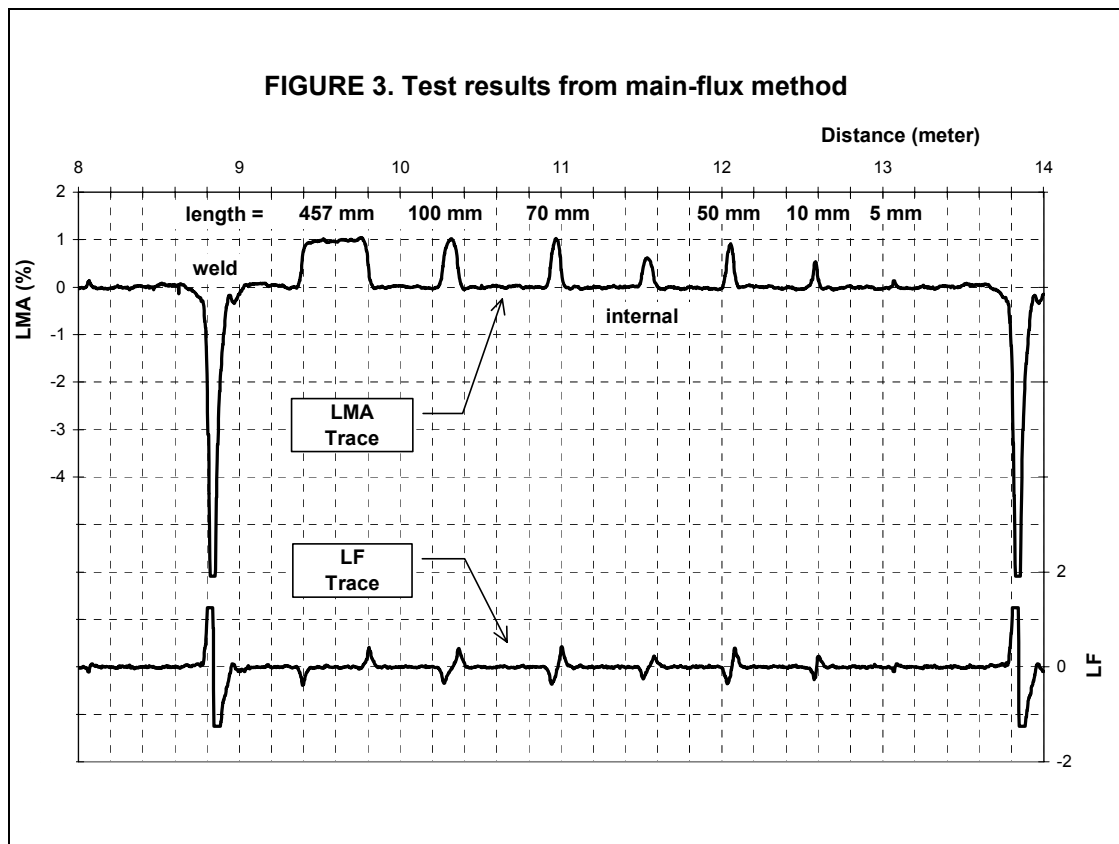
Currently, two generic methods are used for the determination of LMA. They are illustrated in Figure 2.



The **Main-Flux Method** uses an annular coil together with an electronic integrator circuit to determine the local magnetic flux inside the rope (Figure 2a). Note that the coil must encircle the rope. Originally patented¹ in Britain in the 1960s, this approach has been discussed in the literature.^{2, 3, 4} Since it measures the magnetic flux inside the rope locally, the annular coil

approach offers uncommon resolving power, signal fidelity and, therefore, inspection accuracy. The performance of this arrangement is unsurpassed and must be considered the *Gold Standard* by which all other methods are measured.

Unfortunately, it is topologically impossible to implement a hinged annular coil with a large number of turns that can be opened and conveniently attached to the rope. This means, the practical implementation of this method for in-service wire rope inspections is seriously hampered by an inherent and insurmountable problem: An annular coil – encircling the rope – must be wound onto the rope in the field for each inspection. This cumbersome procedure allows only very few turns (say, one hundred) and, hence, only very small induced coil voltages. The coil voltages are of the same order of magnitude as the always-present inherent offset voltages at the input of operational amplifiers that are used for the design of electronic integrator circuits. These inherent offset voltages make the long-term low-drift integration of the coil voltages impossible. Hence, the annular coil approach is not feasible for in-service inspections where LMA measurements over longer time periods – say, over more than a few minutes – are required.



To illustrate the *annular coil* approach, Figure 3 shows the LMA and LF traces of a laboratory test rope. The LMA and LF signals were acquired with an annular coil. Short pieces of wire, attached to the rope, simulate anomalies. The attached wires have different lengths as indicated. They typically represent a 1% increase of metallic cross-sectional area. (The LMA caused by the internal wire is unknown). The two ends of the rope are welded together to form an infinite loop. The weld is also indicated in the chart.

Figure 3 shows the excellent results that could be obtained with annular coils. This means, the increases of metallic cross-sectional area caused by the attached wires are clearly indicated with their full magnitude for wires that are longer than about 50 mm. The metallic cross-sectional area changes caused by shorter wires are also indicated, albeit not to their full extent.

The **Modified Main-Flux Method**, shown in Figure 2b, tries to retain the superior performance of the *Main-Flux Method* while allowing the implementation of hinged sense heads of the *clamshell* design^{3,4}

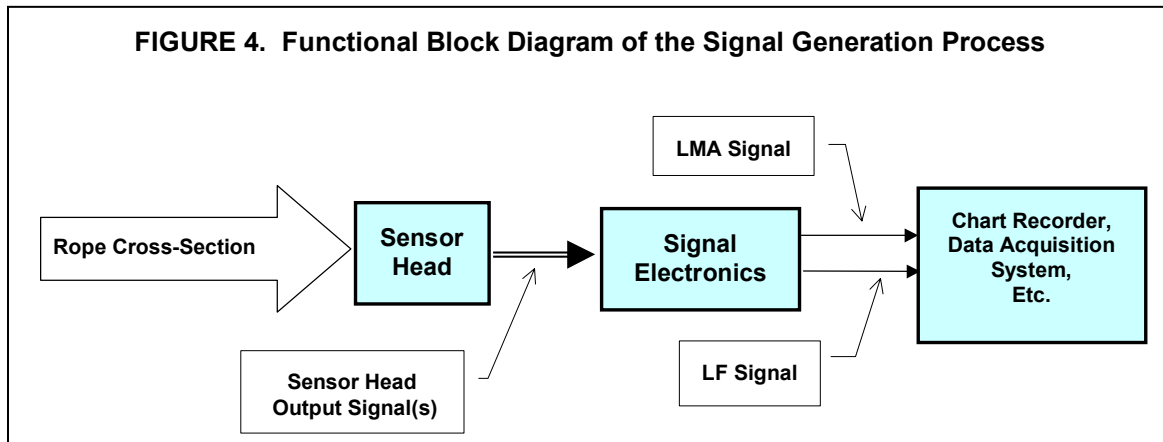
The test signals of this *Modified Main-Flux Method* are a combination of the *Main-Flux* signal and a signal component that is caused by the (parasitic) *outside stray flux*, i.e., that portion of the flux that leaves and enters the sense head to and from the outside, respectively, and flows along some external stray flux path (see Figure 2). Unfortunately, this *outside signal component* is significant. It compromises the quality of the test results and must be considered parasitic. Although this parasitic effect can be minimized,⁵ a true signal of the *main flux* type cannot be completely restored. Nevertheless, the *Modified Main-Flux Method* retains at least some of the desirable features of the *annular coil* approach. In contrast to the above described main-flux approach, the modified main-flux method allows the design of hinged sensor heads of the *clamshell* type. This feature makes it easy to attach the sensor head to the rope even under adverse field conditions.

The **Return Flux Method** uses Hall sensors^{6,7} (or, more complex, fluxgate sensors⁸) to measure the magnetic flux in the magnetic return path of the instrument. Illustrated by Figures 2c and d, the return flux is equal to the *average value of the axial rope flux* inside the sense head plus the *outside stray flux*. Therefore, the return flux provides an estimate of the *average cross sectional area* of that section of the rope that is inside the sense head. Flux sensors can either be inserted into the air gap between the permanent magnet poles and the rope or into the yoke of the magnetizer assembly.

Signal Generation and Evaluation⁵

For the interpretation of test results and for a correlation of test data with the actual rope condition, the rope inspector must understand the capabilities and limitations of his EM rope inspection equipment. A proper appreciation of the signal generation process, together with an understanding of rope degradation mechanisms and discard criteria, is essential for making rational rope retirement decisions. These questions are discussed in the following.

The *Functional Block Diagram* of Figure 4 illustrates the signal generation process. This figure shows the rope's cross-sectional area – including variations caused by broken wires, corrosion, abrasion, etc. – as the input to an EM wire rope inspection system. From this input, the sensor head produces one or several electrical signals. These signals are electronically processed to produce the LF and LMA signals, which are then recorded by a chart recorder and/or stored by a data acquisition system.



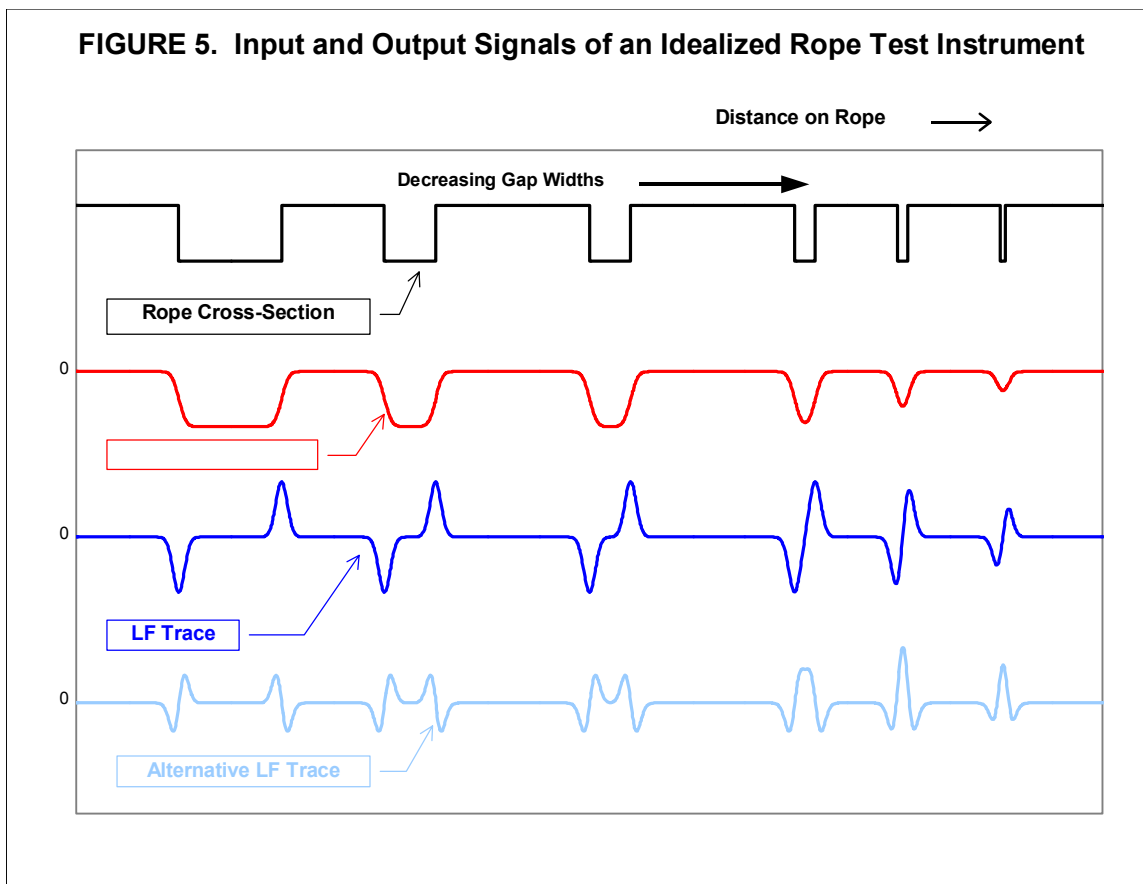
For the following discussion, *step changes of metallic cross-sectional area* – caused by missing or added wires, for example – have particular significance. Because of its simple geometry, a *step change* can be called a *fundamental defect*. Accordingly, the corresponding LMA and LF signals, caused by a *fundamental defect*, can be called *fundamental LMA* or *LF signals*, respectively. The *fundamental signals* can also be called an instrument's *step response*.

It is easy to see that any defect can be represented as the sum of appropriately scaled and spaced *fundamental defects*. Moreover, the process of signal generation is, at least approximately, linear. Hence *linear superposition* applies. This means that, if a defect can be represented as the sum of several *fundamental defects*, then the corresponding defect (LMA and

LF) signals are the sum of the corresponding *fundamental LMA* and *LF signals*. The concepts of fundamental *defects* and *signals*, *step response*, and *linear superposition* are discussed further in the literature.⁹ Determining and evaluating its *step response* is an excellent method for characterizing the performance of an EM wire rope tester.

In the present context, the concept of filtering can be used very loosely. For example, the sensor head of an EM rope tester, together with the signal electronics, may be viewed as a – linear or nonlinear – data filter. This is illustrated further by Figure 5. The figure depicts the rope cross-section as the input signal and the idealized corresponding LMA and LF output signals. Note that, for many rope testers, the LF signal approximates the first derivative of the rope cross-section signal. For other instruments, the LF signal is the second derivative of the rope cross-section, as shown as *Alternative LF Signal* in Figure 5. Note that the signals generated with the *Main Flux Method*, shown in Figure 3, closely resemble the idealized results of Figure 5.

Recognizing differentiation as the quintessential high-pass filter operation, the LF signal can be considered as the rope cross-section input signal that has been high-pass filtered. High-pass filtering accentuates fast changes of signals, and typically broken wires and corrosion pitting cause rapid variations of the rope cross-section. Therefore, the high-pass filtering feature makes the *LF Signal* useful for the detection of broken wires and corrosion pitting.

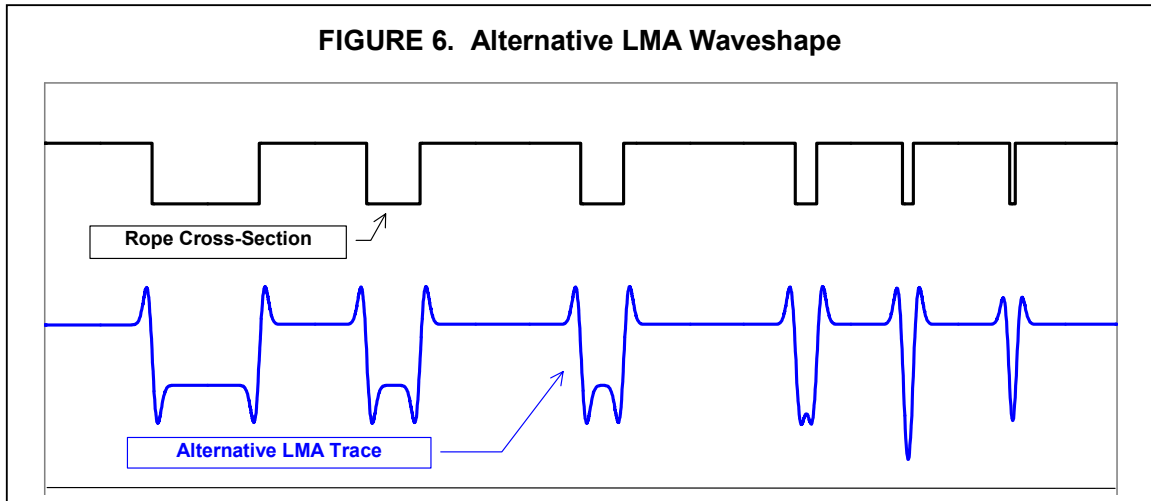


Any inspection equipment should present data in a form that facilitates their interpretation by the human operator. Figure 5 shows that a perfect LMA signal could serve as such an accurate and conceptually simple map of a rope's LMA that is easy to interpret by the inspector.

Unfortunately, actual LMA signals are far from this ideal. Most rope testers can produce LF signals with wave-shapes that are very similar to those of Figure 5. However, producing an LMA signal that comes close to the idealized LMA signal in Figure 5 poses problems.

To illustrate, some EM rope testers produce *LMA step responses* with considerable overshoot in both directions similar to those shown in Figure 6. The overshoot makes LMA

measurements complex, ambiguous and operator dependent. Chart interpretation for these instruments becomes especially problematic under actual field conditions. Because this type of performance is not amenable to analysis, it will not be discussed further.



Resolution and Averaging Length

The dictionary defines *resolution* as “the level of detail that can be distinguished in an image (or a recording).” For electromagnetic wire rope inspections, resolution is always the premier performance measure. In nondestructive testing, the terms *resolution* and *inspection accuracy* are often used synonymously.

In the discipline of electromagnetic wire rope inspection, *quantitative resolution*³ or *averaging length* (sometimes also called *scanning length*) is defined as the minimum length of a uniform anomaly for which the sensor provides an accurate measurement of a rope’s LMA.

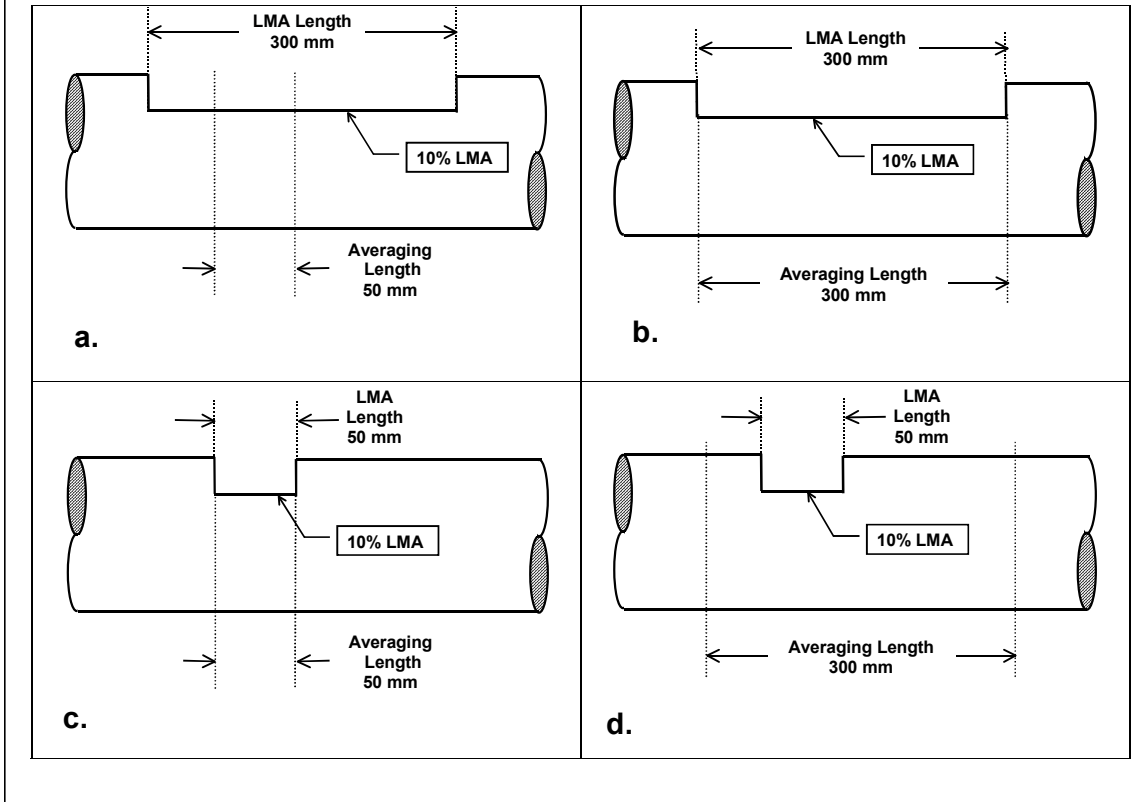
To visualize the concept of *averaging length*, assume that, instead of measuring metallic cross-sectional area directly, the rope tester continuously measures the metallic volume of consecutive rope sections with lengths that are equal to its *averaging length*. Figure 7 illustrates this concept.

Figure 7a shows a (hypothetical) rope with a uniform 10% LMA extending over a length of 300 mm. An instrument with a 50 mm *averaging length* will correctly measure this LMA. As illustrated by Figure 7b, a rope tester with an *averaging length* of 300 mm will also give a true indication of this anomaly.

Now consider a (hypothetical) rope with a 10% uniform LMA extending over a length of 50 mm. Figure 7c shows that an instrument with an *averaging length* of 50 mm can determine the exact LMA caused by this anomaly. However, as can be seen from Figure 7d, an instrument with a an *averaging length* of 300 mm would indicate the same anomaly as a 1.7% LMA extending over a length of 300 mm – a very inaccurate indication of the true rope condition. These examples show the importance of a short *averaging length*.

Note that signal averaging is a quintessential type of low-pass filtering, and that signals lose a significant amount of information (details) by low-pass filtering. Figure 8 illustrates this situation. It shows how the quality of LMA signals deteriorates as the LMA averaging length increases.

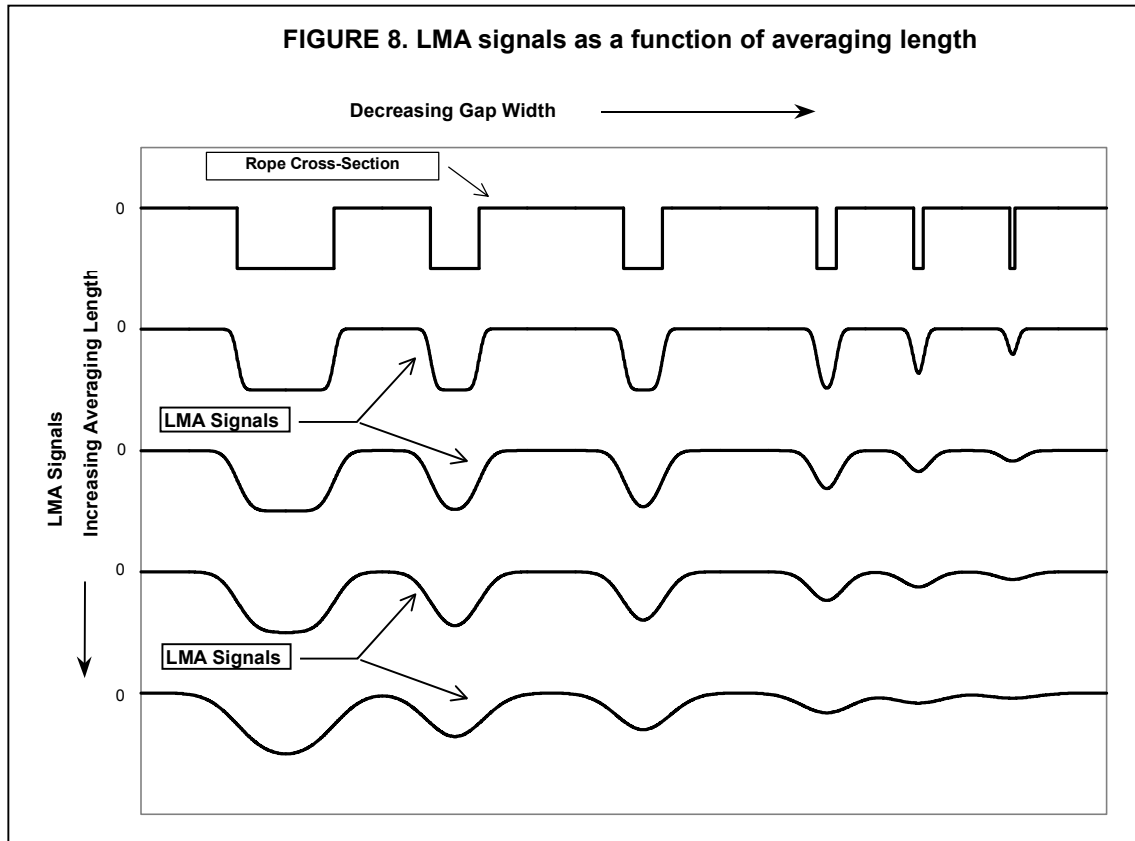
FIGURE 7. LMA length and averaging length



An analogy can illustrate the problems associated with long LMA averaging lengths: A chain is only as strong as its weakest link. Obviously, the strength of a chain is not determined by the average strength of some of its links. Similarly, the strength of a rope, which has lost metallic cross-section by corrosion and/or wear, is determined by the minimum local metallic cross-sectional area along the rope's length, and not by some average value of the rope cross-sectional area.

Experience has shown that serious rope deterioration can occur over very short distances along the length of a rope. Hence, in order to determine and evaluate a rope's actual metal loss with acceptable accuracy, a short *averaging length* – of no more than a few centimeters – is important.

Because all wire rope testers have a *quantitative resolution* or *averaging length* that is greater than zero, an accurate measurement of LMA always requires minimum lengths of anomalies. As the above discussion shows and as illustrated by Figure 8, the concept of *quantitative resolution* or *averaging length* is important for specifying and comparing the performance of rope testers.



Wire Rope Inspection and Retirement

Two different philosophies have been used to effect rope retirement:

1. A *Statutory Life Policy* mandates rope retirement at certain prescribed intervals. (This means, the *Statutory Life Policy* places a maximum on the time a rope can be in service).
2. *Retirement for Cause* is based on retirement conditions that are evaluated periodically by nondestructive inspections. (This means, the Retirement-for-Cause approach requires that the rope must be retired when the deterioration exceeds a certain limit.)

Because a *Statutory Life Policy* is inherently wasteful, regulators have tended to adopt the Retirement-for-Cause approach wherever appropriate.

Wire rope deteriorates gradually throughout its entire service life. To keep abreast of deterioration, wire rope must be periodically inspected. Because moderate deterioration is normally present, the mere detection of rope deterioration does not usually justify rope retirement.

There are two major nondestructive inspection methods for the detection and evaluation of rope degradation: Visual inspections and EM inspections.

Visual Inspection

The rag-and-visual method is a simple yet useful method for detecting a wide variety of external rope deteriorations. Using this approach, the inspector lightly grasps the rope – which moves at inspection speed – with a rag or cotton waste. External broken wires will often porcupine and, as the rope moves, snag the rag or cotton waste. The rope is then stopped at that point, and the inspector assesses the rope condition by a visual examination.

Frequently, broken wires do not porcupine. Then, a different test procedure must be used. The rope is moved two or three feet at a time and visually examined at each stop. This method is tedious and, because the rope is often covered with grease, many external and internal defects elude detection.

Another visual inspection tool is measurement of the rope diameter. Rope diameter measurements compare the original diameter – when new and subjected to a known load – with the current reading under like circumstances. A change in rope diameter indicates external and/or internal rope damage. Inevitably, many sorts of damage do not cause a change of rope diameter.

Several visible signs can indicate distributed losses of metallic cross-sectional area, due to corrosion, abrasion and wear. For example, corrosion products, flattening of outer wires and loss or, sometimes, increase of rope diameter frequently reveal external and internal corrosion. However, the extent of corrosion is often difficult to gauge and its significance is even more difficult to assess.

Visual inspections are inherently not well suited for the detection of internal rope deterioration. Therefore, they have limited value as a sole means of wire rope inspection. However, visual inspections are simple and do not require special instrumentation. When combined with the knowledge of an experienced rope examiner, visual inspection can provide a valuable tool for evaluating many forms of rope degradation.

Electromagnetic Inspections

EM wire rope inspection gives detailed insight into the condition of a rope. Its reliability has made EM testing a universally accepted method for the inspection of wire ropes in mining, for ski lifts, and many other applications.

As discussed, two distinct EM inspection methods have evolved to detect and classify defects of the LMA and LF type.

- *Localized-Flaw Inspection (LF Inspection)*. Like the rag-and-visual method, LF inspection is suited only for the detection of localized flaws, especially broken wires. Therefore, small hand-held LF instruments have been called electronic rags.
- *Loss-of-Metallic-Area Inspection (LMA Inspection)* detects and measures changes of the metallic cross-sectional area caused by wear and corrosion. More reliable than visual diameter checks, LMA inspection can replace diameter measurements made with a caliper. Therefore, LMA instruments could be called electronic calipers.

Electromagnetic and visual wire rope inspections complement each other. Both are essential for safe rope operation, and both methods should therefore be used for maximum safety. The thrust of evolving regulations is clearly toward combined periodic EM and visual inspections

A thorough inspection must consider all aspects of a rope's condition, including:

1. the findings of a visual inspection,
2. the results of an EM rope inspection,
3. the rope's operating conditions and related damage mechanisms,
4. the history of the rope under test and that of its predecessors.

Dependable inspection procedures, using combined visual and EM methods, can detect rope deterioration at its earliest stages. Therefore, wire rope users can employ them as an effective preventive maintenance tool. To illustrate, here are some practical examples.

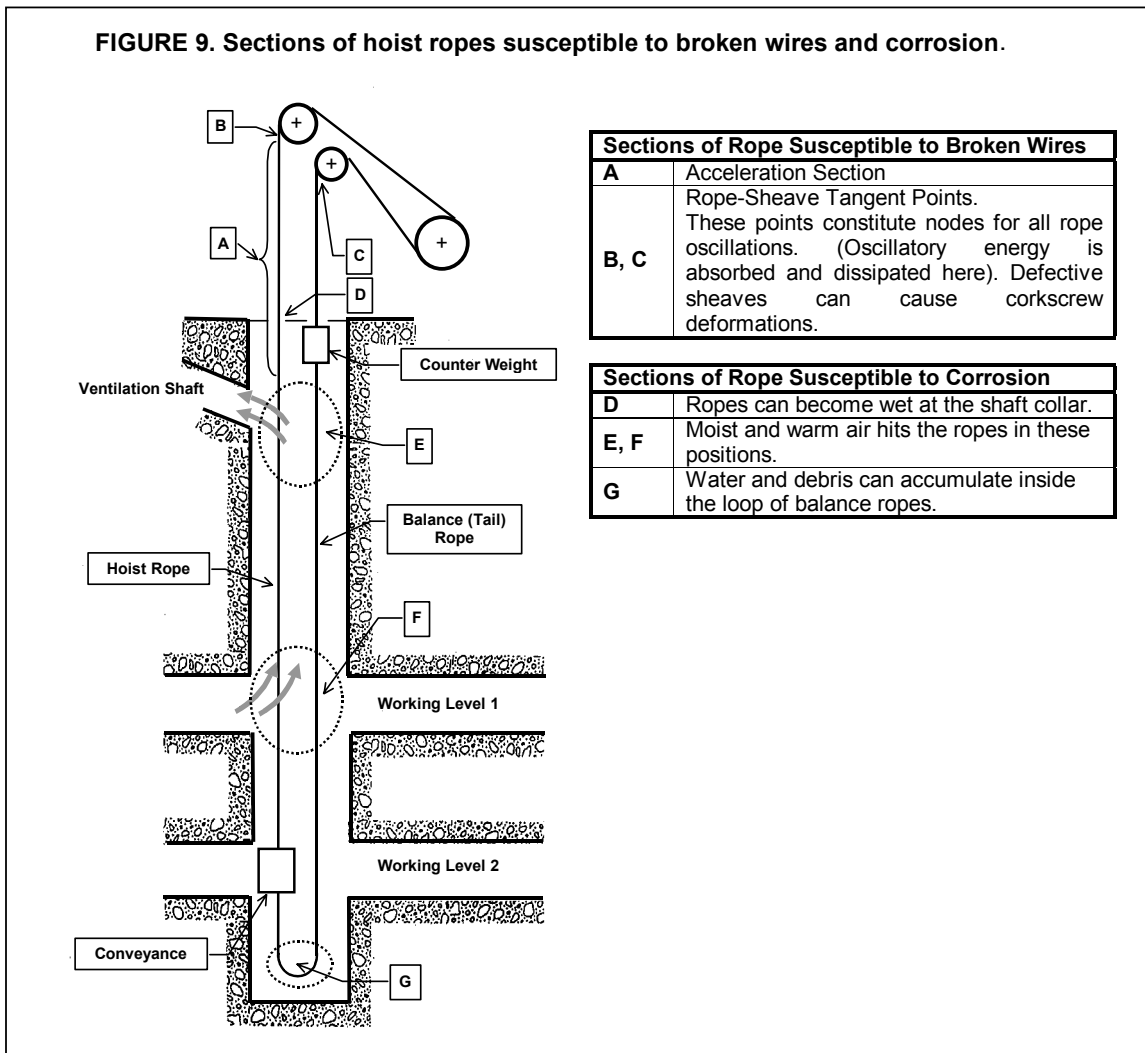
1. The early detection of corrosion allows immediate corrective action through improved lubrication.
2. Accelerating wear and interstrand nicking can indicate a need to reline sheaves to stop further degradation
3. Careful inspections can monitor the development of local damage at the crossover points of the rope on a winch drum. This way, the operator can determine the optimum time for repositioning the rope on the drum.

A program of periodic inspections is especially effective. To establish baseline data for subsequent inspections, such a program should commence with an initial inspection of the installed rope after a certain break-in period. Subsequent inspections should then be performed at scheduled intervals. In particular, periodic EM inspections allow the documentation of a rope's deterioration over its entire service life.

Examples illustrating various types of rope damage, including their associated deterioration mechanisms will be discussed below.

Figure 9 shows the schematic of a mine hoist including sections of mine hoist and balance ropes that are particularly susceptible to rope deterioration.^{10, 11}

FIGURE 9. Sections of hoist ropes susceptible to broken wires and corrosion.



Broken Wires

In running ropes, broken wires develop primarily in sections that move over sheaves, pulleys and winch drums. Typically, they are caused by bending over-sheave fatigue cycling. (See Figure 9, rope sections A, B, C.)

Usually, breaks develop in segments of the rope surface that come into direct contact with the sheave. Here, various contact phenomena compound the fluctuating bending stresses. Breaks in these areas are external and usually visible. However, internal breaks can also develop depending on the loading and, especially, the rope construction. Once broken wires appear, a good many more are likely to develop within a relatively short period.

Corrosion (Rust)

Corrosion is a serious hazard to a wire rope. Corrosion pitting causes stress concentrations. Furthermore, corrosion pitting inhibits the free movement of wires and strands, which produces additional stresses in wires. The increased wire stresses combined with the above mentioned stress concentrations can drastically accelerate the development of fatigue breaks. Wires can also corrode uniformly over their entire surface which may reduce their cross-sectional area and cause loose wires.

Rust can cause shallow pitting on the working surfaces of a rope where the steady rubbing action of the sheave prevents deep cavities. This mechanism accelerates wear. Furthermore, deep corrosion pitting on the internal surfaces of wires can severely shorten service life.

The severity of corrosion often varies along the length of a rope. Frequently, corrosion is localized but, nevertheless, dangerous.

A corrosive environment often exists in certain zones along the length of the mine shaft. Corrosion often occurs in rope sections which stay in these corrosive zones over extended periods.

Corrosive areas are usually located where large and abrupt changes of temperature and/or humidity occur, for example (see Figure 9): below points where water or moist air can enter the shaft; a humid shaft pit; fog areas in ventilation shafts; locations with increased air velocities.

The extent of corrosion is often difficult to gauge and – as shown by experience – usually underestimated. Rust and dirt frequently clog up the rope surface and hide loose wires.

Wear

Wear results in loss of cross-sectional area of the wires. The problems related to external and internal wear require special attention. External wear usually occurs on the working surface of a rope. Severe external wear can indicate that internal wires are similarly worn. Sometimes, severe wear can cause outer wires – or clusters of outside wires – to break abruptly. Rubbing between wires of a strand can cause internal wear.

Deformation and Mechanical Damage

Corkscrew-type deformations can be caused by sheave grooves that are too tight, through manufacturing errors or as a result of severe wear. Corkscrew deformations can cause rope damage by increased exposure to wear. Furthermore, they increase the pressure between adjacent strands, which will eventually cause broken wires.

Kinks are permanent distortions caused by loops that are drawn too tightly. Loops, often precursors of kinks, are formed when a section of a rope under high torsion is allowed to become slack. Usually, ropes with kinks must be removed from service.

A common deterioration mode is peening, also called *plastic wear*, produced by localized impact or very high bearing pressure. This can occur by the slap of the rope at crossover points as the rope slips from layer to layer while winding on multilayer drums at high speeds. Peening sometimes gives the appearance of heavy wear although there is little loss of cross section. Plastic wear can cause a fin on the edge of a worn wire that provides a ready site for the initiation of fatigue cracks.

Mechanical damage can have many causes such as a solid object hitting the rope, improper handling during rope installation, overloading or shock loading. Usually, mechanical damage is clearly visible and easy to detect. However, some forms of mechanical damage, such as *wire plucking*, can be more difficult to locate. (Wire plucking is mechanically equivalent to guitar string plucking.) Lateral scraping of the rope at cross-over points on a winch drum frequently causes this damage mechanism. It can lead to localized damage in the form of one or several broken wires at set intervals along the rope

Martensitic Embrittlement

Martensite is a brittle phase of steel formed, for example, when the steel is heated above a critical temperature and then rapidly quenched. It occurs in wire rope as a result of frictional surface heating and the mass cooling effect of the cold metal beneath. Martensitic embrittlement can develop at rope crossover points while winding on multilayer drums. Here the rope can be heated by contact with the adjacent turn and then rapidly quenched by the surrounding metal. Martensite cracks easily, and such cracks can propagate from the surface through the entire wire.

Combined Deterioration Modes

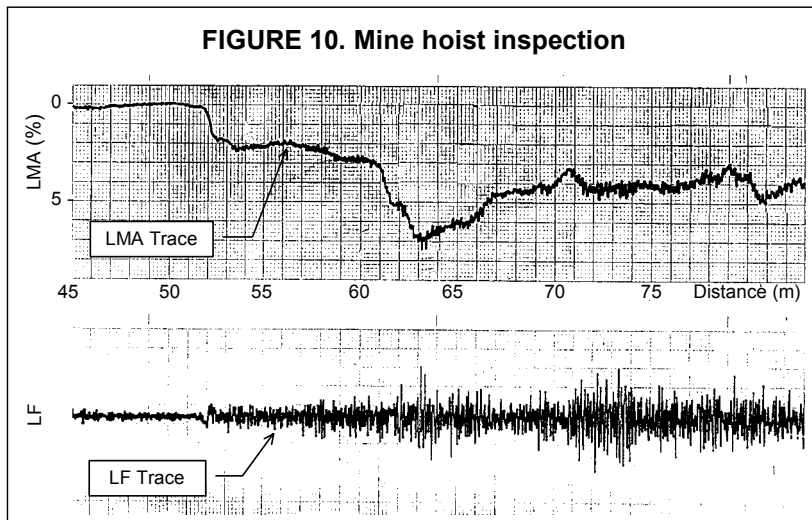
In practice, combined deterioration modes predominate. These include corrosion fatigue and corrosion-assisted wear. Typically, one type of rope degradation can initiate and ferment interactive deterioration mechanisms.

Corrosion-assisted wear is probably the most common deterioration mode in stranded mine hoist ropes. While broken wires do occur, the majority of mine hoist ropes is retired due to unacceptable LMA rather than broken wires,

Often, metal loss is caused by internal corrosion and abrasion which are not visible from the surface. As the various deterioration mechanisms progress, they will eventually cause broken wires or clusters of broken wires.

Example 1. Mine hoist rope inspection

Figure 10 is an EM inspection chart of a mine hoist rope that shows the typical wear-fatigue chart patterns caused by bending over a sheave combined with acceleration and deceleration of the conveyance (see Figure 9). The upper part of the recording shows the LMA trace. The lower part shows the LF trace. Distance scaling is shown on the bottom margin of the LMA recording.



The rope section whose chart recording is shown to the left in Figure 10 – up to a rope distance of approximately 52 m – shows no deterioration. This section is located directly above the conveyance (or counterweight) and, therefore, never moves over the head sheave.

The recording shows corrosion, including corrosion pitting, and broken wires starting at a rope distance of approximately 52 m. This

is the point where the rope just contacts the sheave when the conveyance is at the shaft collar.

This typical pattern of rope damage can be explained as follows. When the conveyance starts at the bottom of the shaft, the rope-conveyance arrangement develops rather slow longitudinal, lateral and torsional oscillations. When the conveyance reaches the top of the shaft, the initially low frequency oscillations become high-frequency vibrations. The stopping and acceleration action of the conveyance at the shaft collar causes additional vibrations.

The tangent point of the rope and the sheave constitutes a node for all rope oscillations. These oscillations induce considerable tension, bending and torsional stresses at the tangent point. The oscillatory energy in the rope is dissipated and absorbed at this node. This action induces fatigue and abrasion at the tangent point.

Furthermore, as shown in Figure 9, condensation water can form at the shaft collar. This, together with the fatigue damage, can cause fatigue-corrosion in this section of the rope.

The LF trace confirms the indications of the LMA trace. In particular, the LF trace indicates considerable corrosion pitting.

This rope shows a maximum LMA of about 7.5%. According to the most common retirement criteria*, a rope must be retired when its LMA exceeds 10% of cross-section. Therefore, the condition of this rope can still be considered acceptable although the chart indicates considerable degradation.

Note that for this example the best and the worst section for this rope are next to each other. This allows an easy comparison of the most degraded rope section with the rope in its, essentially, new condition. Fortunately, this situation is true in many cases, which greatly facilitates rope evaluation.

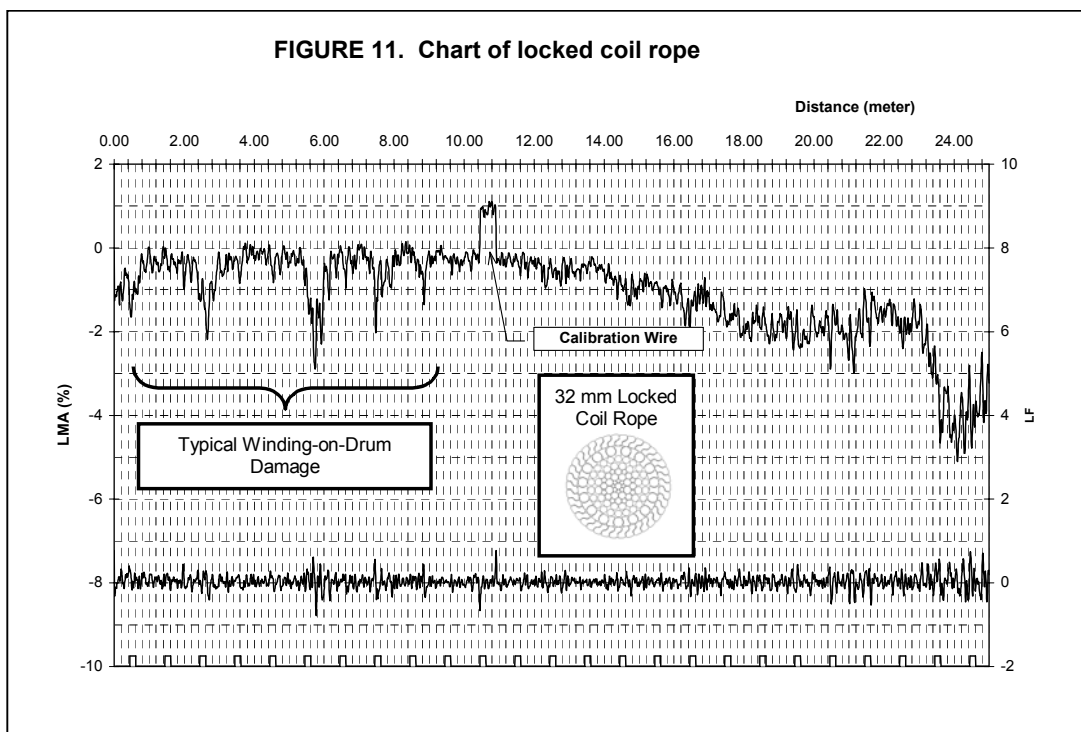
* At this point, retirement criteria that are based on EM rope inspections are still subject to considerable discussion and not universally accepted.

Example 2. Winch rope inspection¹²

This locked coil rope was mounted on a mobile winch for approximately 10 years after 3 months earlier use on a friction winder installation. Its cross-sectional diagram is shown as part of Figure 11. The rope showed clear evidence of external corrosion, variable along the test length. Using retirement criteria that are appropriate for visual inspections, this rope would have been rejected for further use. Due to its service history the rope was not believed to contain any internal local defects.

Examination after Dismantling. After dismantling, the rope showed severe corrosion on the outer layer and also significant corrosion on the second layer. The third layer showed less corrosion, and from the fourth layer onward the rope appeared undamaged, because lubricants were still present. No local defects were found.

Findings of Electromagnetic NDT Inspection. Figure 11 shows an EM chart of this rope. The maximum measured LMA is 5.1% compared to the best section on the rope covered by the chart.



Note that the most convenient calibration method for EM inspections is to attach a calibration wire with known cross-sectional area to the rope. In the present case a wire bundle that represents about a 1% increase in rope cross-section was taped to the rope and used for calibration. This is indicated in the chart of Figure 11.

The chart shows variable corrosion, corrosion pitting and, possibly, broken wires. As discussed previously, the slap of the rope at the crossover points can cause peening, martensitic embrittlement and/or wire plucking with the associated rope damage as the rope crosses over from layer to layer on a drum. The deterioration pattern indicated to the left of the chart is typical for ropes that wind on a drum with the worst deterioration occurring at the crossover points as the rope slips from layer to layer while winding on a multilayer drum.

FIGURE 12. Construction of multistrand ropes



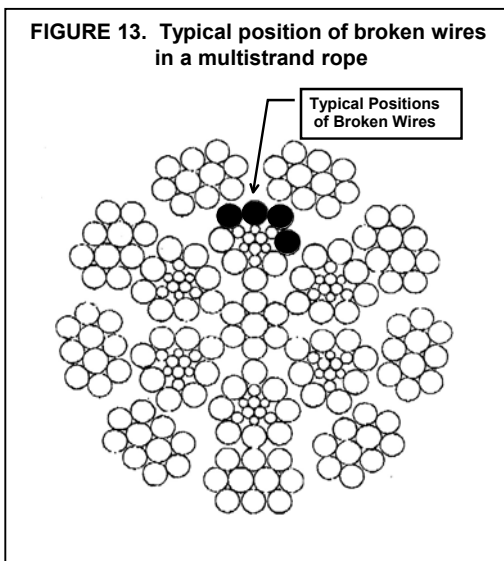
Multistrand ropes^{13, 14}

Many ropes are of the torque-balanced multistrand type comprising two or more layers of strands. Figure 12 shows a cutaway section of such a rope. Torque balance is achieved in multistrand ropes by laying outer and inner strands in opposite directions.

This type of rope construction limits axial rotation of the freely suspended rope under load. In addition, multistrand ropes offer flexibility and a wear resistant surface profile.

However, the wires and strands in different layers of these ropes touch locally and at an angle. Therefore, when multistrand ropes bend over sheaves or on a drum, they are subject to the combined effect of radial loading, relative motion between wires and bending stresses. This causes fretting wear or fatigue and interwire nicking across the interface between layers.

FIGURE 13. Typical position of broken wires in a multistrand rope



Therefore, multistrand ropes are prone to develop internal broken wires. This breakup occurs primarily on the interface between the outer and second layer of strands, usually with no externally visible signs (see Figure 13). The wires in the second layer of strands typically show interstrand nicking and breaks caused by a combination of fluctuating axial wire stresses, inter-wire motions and fluctuating radial loads. The broken wires usually show squared-off and z-shaped ends that are typical for fatigue breaks.

Many multistrand ropes are subject to corrosive environmental conditions. For example, offshore ropes are either immersed in the sea or continually wetted by salt water spray. In addition, heavy use in a marine environment can displace and degrade the rope lubricant. The combined effects of fatigue, corrosion and lubricant degradation can cause rapid internal deterioration

where there is no effective form of protection.

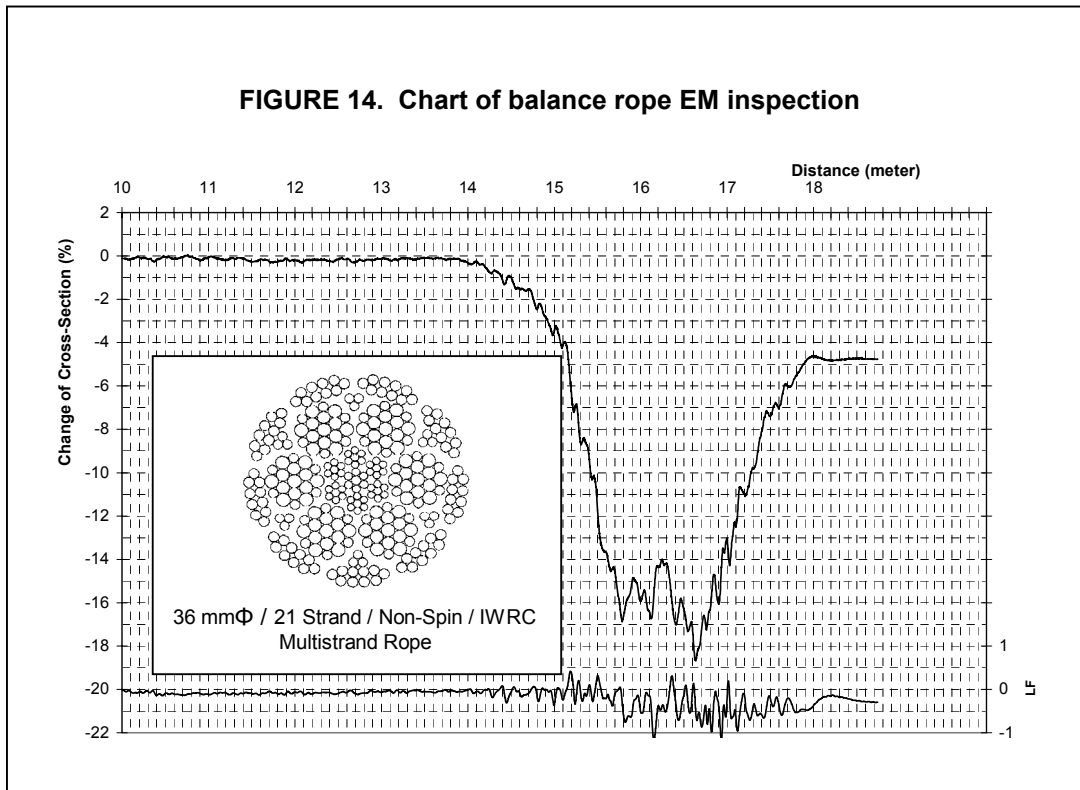
Example 3. Balance rope inspection¹⁵

Figure 14 shows an EM inspection chart recording of a mine balance rope (see Figure 9). Note that frequently torque-balanced ropes of the multistrand type are used as balance ropes because regular stranded ropes develop internal torques during operation. Since balance ropes are under very little tension, internal torques in ropes can cause loops, which are often precursors of kinks. Ropes with kinks must be removed from service. The use of multistrand ropes avoids this problem.

Figure 14 shows the typical corrosion chart pattern caused by the accumulation of water and debris inside the loop (see Figure 9) of a multistrand balance rope. Water and debris are especially prone to accumulate inside this loop while the conveyance is parked at the shaft collar over extended time periods. A cross-sectional diagram of this rope is also shown as part of Figure 14. Note that, as in Example 1, the chart shows the best rope section – essentially with no rope deterioration – right next to the worst section. This feature greatly facilitates rope evaluation.

The chart shows an LMA of 19%, which clearly calls for rope retirement. A subsequent destructive break test showed a loss of breaking strength of 48.3% for the worst rope section. On the other hand, the cross-sectional area of the second layer of strands represents about 47% of the total rope cross-section. This suggests that the second layer of strands has completely lost all load-bearing capability.

FIGURE 14. Chart of balance rope EM inspection



Example 4. Experimental multistrand rope inspection¹⁵

This case study illustrates the use of EM wire rope inspections for the detection and quantitative characterization of internal broken wires and clusters of broken wires. The present experiment deals with the inspection of a torque balanced multistrand rope with no corrosion and many broken wires. This rope has been used as a mine hoist rope on a trial basis and was known to contain numerous internal broken wires along its entire length.

The task at hand was to determine the number of broken wires in 100 mm segments along the length the rope. The difficulty of this quantitative defect characterization problem was compounded by the fact that an undamaged rope section – usually the segment directly above the conveyance – was not available for comparison. Further, at the time, the correlation of the typical deterioration modes of this and similar ropes with their EM inspection results was generally not well understood.

A cross-sectional diagram of this multistrand rope is shown in Figure 13. As indicated in the figure, it is known that broken wires in multistrand ropes usually develop in the second layer at the interface between the first and the second layer of strands. In addition, from this and similar ropes' service histories, it can be assumed that the rope under inspection has developed significant interstrand nicking together with numerous fatigue breaks of wires in the second layer of strands.

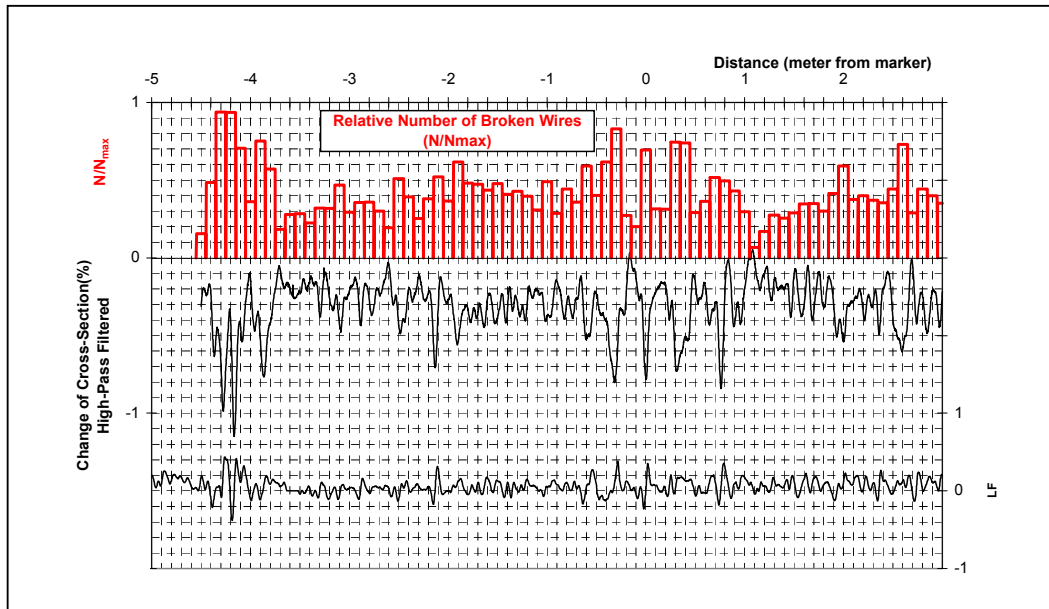
The detailed detection and quantitative characterization of internal broken wires in ropes with many breaks and clusters of breaks – such as the present rope – pose problems. Difficulties are caused by the fact that, for electromagnetic wire rope inspections, the indication of a broken wire is influenced by a number of parameters like

- a) broken wire cross-sectional area,
- b) broken wire gap width, and
- c) by the position of the broken wire within the cross-section of the rope.
- d) For clusters of broken wires, an additional problem is caused by the fact that the relative position of broken wires with respect to each other along the length of the rope is not known. For example, the gaps of broken wires could be aligned or staggered.

e) Finally and most importantly, broken wires with zero or tight gap widths are not detectable by electromagnetic inspections because they do not produce a sufficient magnetic leakage flux. Considering the above, only an estimate of the number of broken wires is possible.

Conventionally, the LF trace is used for the detection of broken wires. However, the LF signal is not quantitative and can not be used for estimating the number of broken wires. On the other hand, the LMA trace of the inspection chart in Figure 15 shows rapid relatively small variations of cross-section. These variations are significant and can be used to estimate the number of broken wires per unit of rope length. Note, however, that the *averaging length* or *quantitative resolution* of the instrumentation used must be sufficient to allow this quantitative defect characterization.

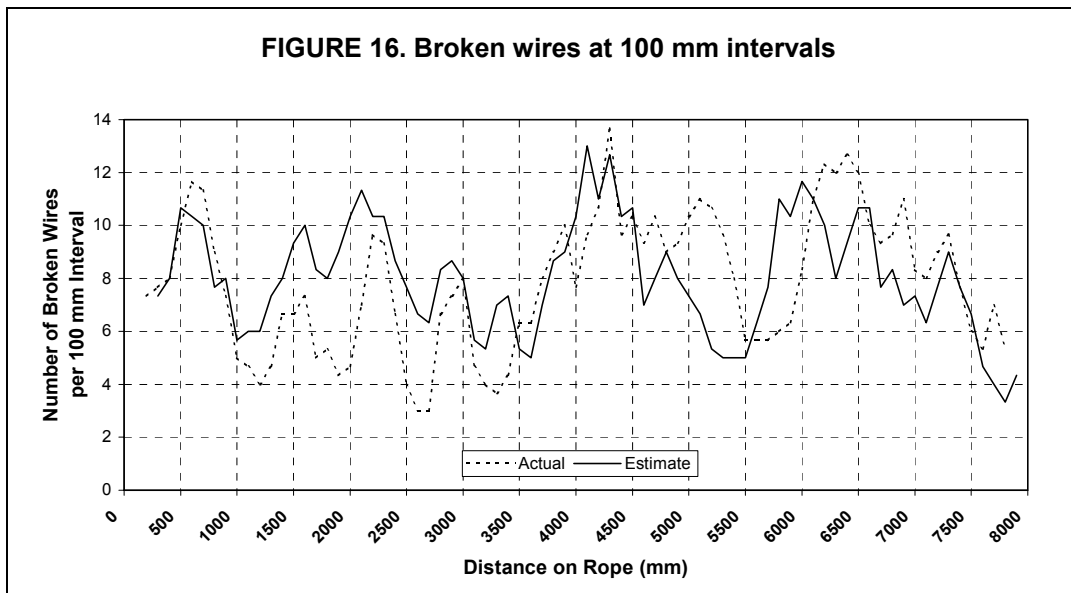
The estimated number of broken wires per 100 mm of rope length, N , derived from the LMA trace, is shown on the top of Chart 15. Here, N_{max} denotes the maximum number of broken wires per 100 mm of rope length. Based on the operating history of this and similar ropes, a value of $N_{max} = 20$ can be estimated.



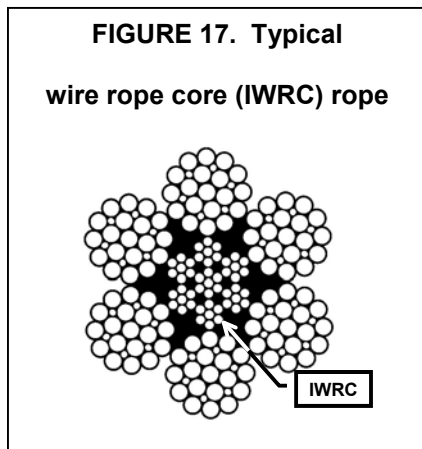
The rope was subsequently disassembled to determine the actual number of broken wires per unit of rope length. Broken wire estimates together with the actual number of broken wires along the length of the rope are shown in Figure 16. Considering the fact that the LMA trace not only indicates broken wires but also interstrand nicking, internal wear and other disturbances of the rope structure, there is a good correlation between the actual and estimated number of internal broken wires. The correlation between actual and estimated number of broken wires up to a rope distance of about 4500 mm is very good. Beyond this distance, there is an offset, which is probably due to a distance measurement error during disassembly of the rope.

A subsequent destructive break test of the rope showed a 30.2% loss of breaking strength. On the other hand, the second layer of strands of the rope (see Figure 13) represents about 30% of the total rope cross-sectional area. Similar to Example 3, this leads to the hypothesis that, for this rope, the second layer of strands has lost all load-bearing capability.

The lack of sufficient information on the rope's operating history – and that of its predecessors – made this rope evaluation particularly difficult. Under normal circumstances, these details are known and must be considered when assessing the rope condition. Altogether, this evaluation shows that a quantitative defect characterization for ropes with internal broken wires and clusters of broken wires is possible. The example illustrates the capabilities and limitations of EM wire rope inspection methods for this particular defect characterization problem.



Example 5. Mooring rope inspection



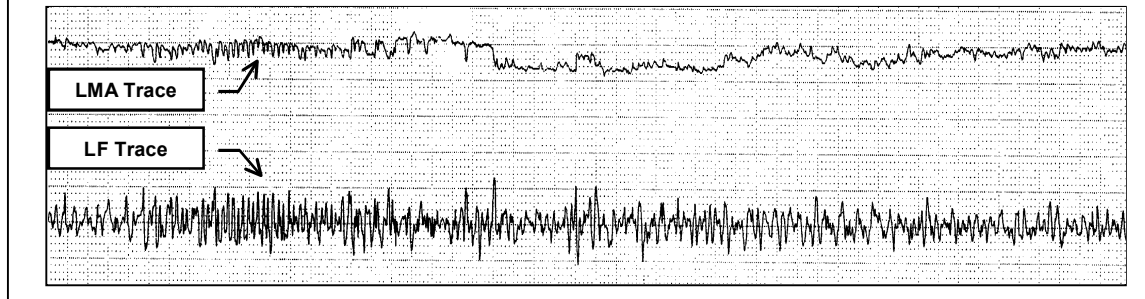
This example deals with the inspection of an IWRC (Independent Wire Rope Core) mooring rope with a diameter of 89 mm whose inspection is depicted in Figure 1.

Figure 17 shows a typical cross-sectional diagram of such a rope. For IWRC ropes, the outer wires of the outer strands have a larger diameter than the outer core strand wires. To minimize interstrand nicking between the outer strands and the IWRC, these ropes are designed such that the wires of the outer strands and the IWRC are approximately parallel. (This is usually achieved by choosing a *lang lay* construction for the IWRC and an *ordinary lay* construction for the outer strands.¹⁰) Typically, the wires of the outer strands are well supported by their neighbors while the outer wires of the IWRC are relatively unsupported.

The result of these geometrical features is that, under fluctuating tensile loads, the outer IWRC wires are continuously forced into the valleys between the outer strand wires and then released. This mechanism results in secondary bending stresses in the core wires leading to large numbers of fatigue breaks. These breaks can be very close together and can form groups of breaks. Eventually, the IWRC can completely disintegrate into short pieces of wire about half a lay length long.

Figure 18 shows the results of the present mooring rope inspection. The chart recording indicates a severe breakup of the independent wire rope core, which is strong evidence of heavy fluctuating tensile fatigue loading. Note that the LMA and LF traces show the typical patterns of broken and missing wires (see Figure 5). The *missing wire* patterns even indicate that short pieces of broken IWRC wires might have fallen out of the rope. In addition, together with the findings of a visual inspection, the chart indicates severe corrosion, including corrosion pitting. Note that corrosion products are clearly visible in Figure 1.

FIGURE 18. Inspection chart of 89 mm IWRC mooring rope with corrosion and severe core damage



REFERENCES

1. Whitehead, E.A.N. "Method of Obtaining an Electrical Signal Proportional to the Cross-Sectional Area of a Magnetic Tube or Rod," UK Patent 913,780 (December 1962).
2. Rieger, W. "Ein Beitrag zur magnetinductiven Querschnittsmessung von Drahtseilen" ("A Contribution to the Magnet-Inductive Cross-Sectional Area Measurement of Wire Ropes"), Doctoral Dissertation, Universität Stuttgart, Germany (1983).
3. Weischedel, H.R. "The Inspection of Wire Ropes in Service, A Critical Review." *Materials Evaluation*. Vol. 43, No.13. American Society for Nondestructive Testing, pp. 1592-1605.
4. Weischedel, H.R. "Method and Apparatus for Magnetically Inspecting Elongated Objects for Structural Defects." US Patent 4,659,991 (April 1987).
5. Weischedel, H.R. "Electromagnetic Wire Rope Inspection: Signal Generation, Filtering, and Computer-Aided Rope Evaluation." Presented at *The Nondestructive Testing of Rope*. Krakow, Poland: (O.I.P.E.E.C.) International Organization for the Study of the Endurance of Wire Rope. (September 1999)
6. Kitzinger, F. and G.A. Wint. "Magnetic Testing Device for Detecting Loss of Metallic Area and Internal and External Defects in Elongated Objects." US Patent 4,096,437 (June 1978).
7. Marchent, B.G. "Apparatus for Nondestructive Testing of Elongate Objects." UK Patent Application GB 2 012 966 (December 1978).
8. Tomaiuolo, F.G. and J.G. Lang. "Method and Apparatus for Nondestructive Testing of Magnetically Permeable Bodies Using a First Flux to Saturate the Body and a Second Flux Opposing the First Flux to Produce a Measurable Flux." US Patent 4,495,465 (January 1985)
9. Weischedel, H.R. "Quantitative In-Service Inspection of Wire Ropes, Applications and Theory." *International Advances in Nondestructive Testing*, Vol. 15, New York: Gordon and Breach Science Publishers (1990): p. 83 – 118.
10. *Wire Rope Users Manual*, Third Edition. Woodstock, MD: Wire Rope Technical Board (1993).
11. Weischedel, H.R. "The Inspection of Mine Hoist Ropes." *Wire Rope News & Sling Technology*. Vol. 12, No. 5. Colonia, NJ: VS Enterprises (June 1991) : p 14-25.
12. Smith, D.T. and P. McCann. *Evaluation of Instruments for the Non-Destructive Testing of Wire Ropes*. Report Number FE/02/07. Buxton, Derbyshire. UK: Health & Safety Laboratory (2002)
13. Weischedel, H.R. and C.R. Chaplin. "Inspection of Wire Ropes for Offshore Applications." *Materials Evaluation*. Vol. 49, No. 3. The American Society for Nondestructive Testing (1991): p. 362-367.
14. Weischedel, H.R. and C.R. Chaplin. "The Inspection of Offshore Wire Ropes: The State of the Art." Paper OTC 6969. Presented at *Offshore Technology Conference*. Houston, TX: (May 1992).

15. Dohm. M. *An evaluation of international and local magnetic rope testing instrument defect detection capabilities and resolution, particularly in respect to low rotation, multilayer rope constructions.* Project Number GAP 503 and GAP 353. Johannesburg, South Africa: Safety in Mines Research Advisory Committee (1999).